ELSEVIER

Journal of Volcanology and Geothermal Research 91 (1999) 1–21

Journal of volcanology and geothermal research

www.elsevier.com/locate/jvolgeores

Tungurahua Volcano, Ecuador: structure, eruptive history and hazards

Minard L. Hall [a,1], Claude Robin [b,*], Bernardo Beate [c], Patricia Mothes [a,1], Michel Monzier [a,d,2]

[a] *Instituto Geofísico, Escuela Politécnica Nacional, P.O. Box 1701-2759, Quito, Ecuador*

[b] *Institut de Recherches Pour le Développement (IRD, ex-ORSTOM), UR 6, OPGC, 5 Rue Kessler, 63038, Clermont-Ferrand, France*

[c] *Departamento de Geología, Facultad de Geología, Minas y Petróleos, Escuela Politecnica Nacional, P.O. Box 1701-2759, Quito, Ecuador*

[d] *Institut de Recherches pour le Développement (IRD, ex-ORSTOM), UR 6, A.P. 17-11-6596, Quito, Ecuador*

Accepted 25 March 1999

Abstract

Tungurahua, one of Ecuador's most active volcanoes, is made up of three volcanic edifices. Tungurahua I was a 14-km-wide andesitic stratocone which experienced at least one sector collapse followed by the extrusion of a dacite lava series. Tungurahua II, mainly composed of acid andesite lava flows younger than 14,000 years BP, was partly destroyed by the last collapse event, 2955 ± 90 years ago, which left a large amphitheater and produced a ~ 8-km^3 debris deposit. The avalanche collided with the high ridge immediately to the west of the cone and was diverted to the northwest and southwest for ~ 15 km. A large lahar formed during this event, which was followed in turn by dacite extrusion. Southwestward, the damming of the Chambo valley by the avalanche deposit resulted in a ~ 10-km-long lake, which was subsequently breached, generating another catastrophic debris flow. The eruptive activity of the present volcano (Tungurahua III) has rebuilt the cone to about 50% of its pre-collapse size by the emission of ~ 3 km^3 of volcanic products. Two periods of construction are recognized in Tungurahua's III history. From ~ 2300 to ~ 1400 years BP, high rates of lava extrusion and pyroclastic flows occurred. During this period, the magma composition did not evolve significantly, remaining essentially basic andesite. During the last ~ 1300 years, eruptive episodes take place roughly once per century and generally begin with lapilli fall and pyroclastic flow activity of varied composition (andesite + dacite), and end with more basic andesite lava flows or crater plugs. This pattern is observed in the three historic eruptions of 1773, 1886 and 1916–1918. Given good age control and volumetric considerations, Tungurahua III growth's rate is estimated at ~ 1.5×10^6 m^3/year over the last 2300 years. Although an infrequent event, a sector collapse and associated lahars constitute a strong hazard of this volcano. Given the ~ 3000 m relief and steep slopes of the present cone, a future collapse, even of small volume, could cover an area similar to that affected by the ~ 3000-year-old avalanche. The more frequent eruptive episodes of each century,

* Corresponding author. E-mail: robin@opgc.univ-bpclermont.fr

[1] E-mail: geofisico@accessinter.net.

[2] E-mail: geofisico@accessinter.net, michmari@orstom.org.ec.

0377-0273/99/$ - see front matter
PII: S0377-0273(99)00047-5

characterized by pyroclastic flows, lavas, lahars, as well as tephra falls, directly threaten 25,000 people and the Agoyan hydroelectric dam located at the foot of the volcano.

Keywords: Andesite magmatism; Debris avalanche and dam; Magma flux rate; Hazards; Tungurahua Volcano; Ecuador

1. Introduction

Tungurahua Volcano (Lat. 01°28′S; Long. 78°27′W) is located on the Eastern Cordillera of the Ecuadorian Andes, 120 km south of Quito and 33 km southeast of Ambato, the capital of Tungurahua Province (Fig. 1). This 5023-m-high active volcano is notable for its extreme relief (3200 m), steep sides, and small summit glacier. Along with other large active volcanoes such as Cotopaxi, Sangay, Antisana and Cayambe, it defines the eastern volcanic row in Ecuador, some 35 km behind the volcanic front that lies on the Western Cordillera.

Early geological and petrographical descriptions of Tungurahua were given by Reiss (1874), Stübel (1886), Wolf (1892) and Reiss and Stübel (1904). More modern studies of the volcano and its hazards were carried out by Salazar (1977), Hall and Vera (1985, Hall and Hillebrandt (1988) and Almeida and Ramon (1991). According to the catalogue of active volcanoes (Simkin and Siebert, 1994), this volcano has experienced 17 eruptions since its discovery in

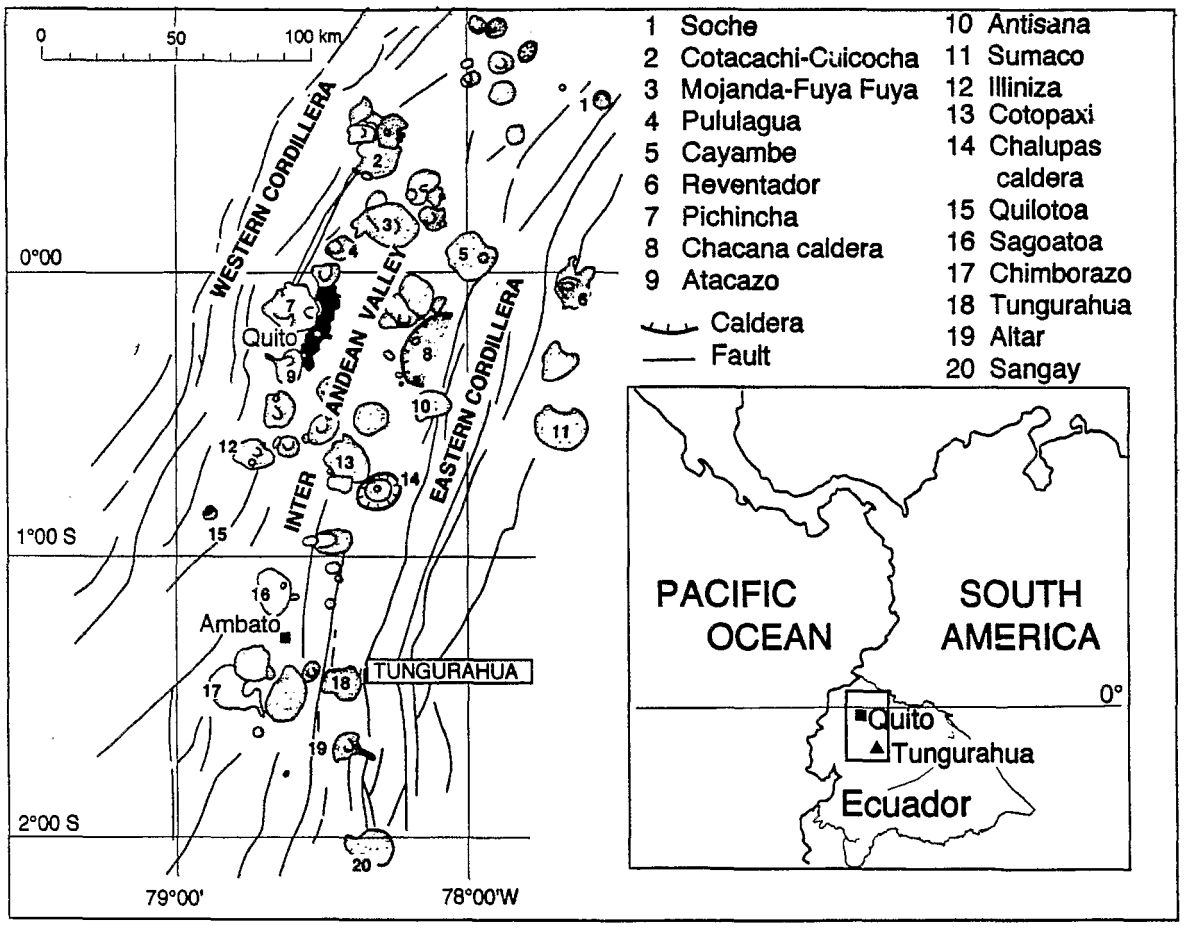

Fig. 1. Location of Tungurahua Volcano. The names of the 20 main Quaternary volcanic edifices are given.

1532, 10 of them being uncertain. Four major eruptive episodes are recognized by historical reports: in 1641–1646, 1773–1781, 1886–1888 and 1916–1918, the former needing to be confirmed. In total, they amount to seven major emissions of lava, pyroclastic flows and fallout tephra. The development and consequences of the two largest historic eruptions, those of 1886 and 1916–1918, were described in considerable detail by A. Martinez (1886) and N. Martinez (1932). Additionally, crater explosions occurred in 1797, coinciding with the earthquake that destroyed nearby Riobamba. Increased fumarolic activity was reported in 1857, and in 1873, 1877, 1883 and 1885, apparently preceding the eruption of 1886. After the 1916–1918 eruptive period, important fumarolic activity continued until 1925. Fumaroles still exist along the northern edge of the present summit crater (150–200 m in diameter and 50 m deep) and hot springs occur around the base of the volcano.

2. Focus of the study

Because of its numerous eruptions, the widespread ash deposits around the cone, and the frequent generation of pyroclastic flows and lahars, Tungurahua is considered to be a dangerous volcano which threatens the tourist town of Baños, as well as other small villages (Fig. 2). A few kilometers east of Baños, the large Pastaza river is contained by the Agoyan dam and used for hydroelectric power generation. Future eruptions of Tungurahua threaten this dam and reservoir, the second most important in Ecuador.

Unfortunately, historical reports concerning Tungurahua's early eruptions are commonly brief and unclear, making it difficult to correlate eruptive events with the tephra stratigraphy, especially without 14C dates and petrological support. As an example, pyroclastic flow deposits attributed to the 1641 AD eruption by Almeida and Ramon (1991) were dated by us at more than 1000 years BP. Moreover, Egred (1989) questions the authenticity of the 1641 eruption. The aim of the present paper is to provide an overall view of the recent volcanic development of this little known volcano and will focus on the Holocene and Historic eruptive activity, including the last sector collapse. This study is based on work carried out before 1989 which was written in Spanish and only available locally (INECEL, 1989), on fieldwork carried out in 1995–1997, and the study of about 50 stratigraphic sections, 11 of which are presented here. A petrological study based on 90 whole-rock analyses will be the focus of another paper. Here, only the broad petrographic nature of the volcanic units is presented to help the reader in understanding the volcanic history.

3. Overall structure

The Tungurahua volcanic complex was constructed upon the Paleozoic–Cretaceous regional metamorphic basement that underlies the Eastern Cordillera (Litherland and Egüez, 1993). It has a broad conical form with a basal diameter of 14 km. The surrounding topography varies between 2000 and 3000 m in elevation and the principal rivers that encircle the cone—the Chambo, Puela and Pastaza rivers—descend from 2400 to 1600 m elevation (Fig. 2).

The complex consists of three successive edifices, the two former ones have been partially destroyed by large sector collapses: (i) the northern, eastern and southern flanks belong to the older edifice of Tungurahua I, which is represented today by large, outwardly-dipping surfaces that are not graded to the present cone and are greatly incised by deep canyons (Fig. 3); (ii) the intermediate cone of Tungurahua II, now only represented by a series of lava flows on the upper southern flank; and (iii) the young edifice, a near-symmetrical cone with steep 30–35° slopes, occupies the western third of the older volcanic complex, nearly filling the avalanche amphitheater carved into the west flank by the last sector collapse event. Incipient erosion has cut gorges only 10–40 m deep into this cone.

4. Main stages of development

4.1. Older Tungurahua (Tungurahua I)

Immediately south of Baños the northern remnant flanks of Tungurahua I consist of a ~400-m-thick concordant series of basic andesitic and andesitic lava flows (55.0–58.6 wt.% SiO_2; see Table 1) and

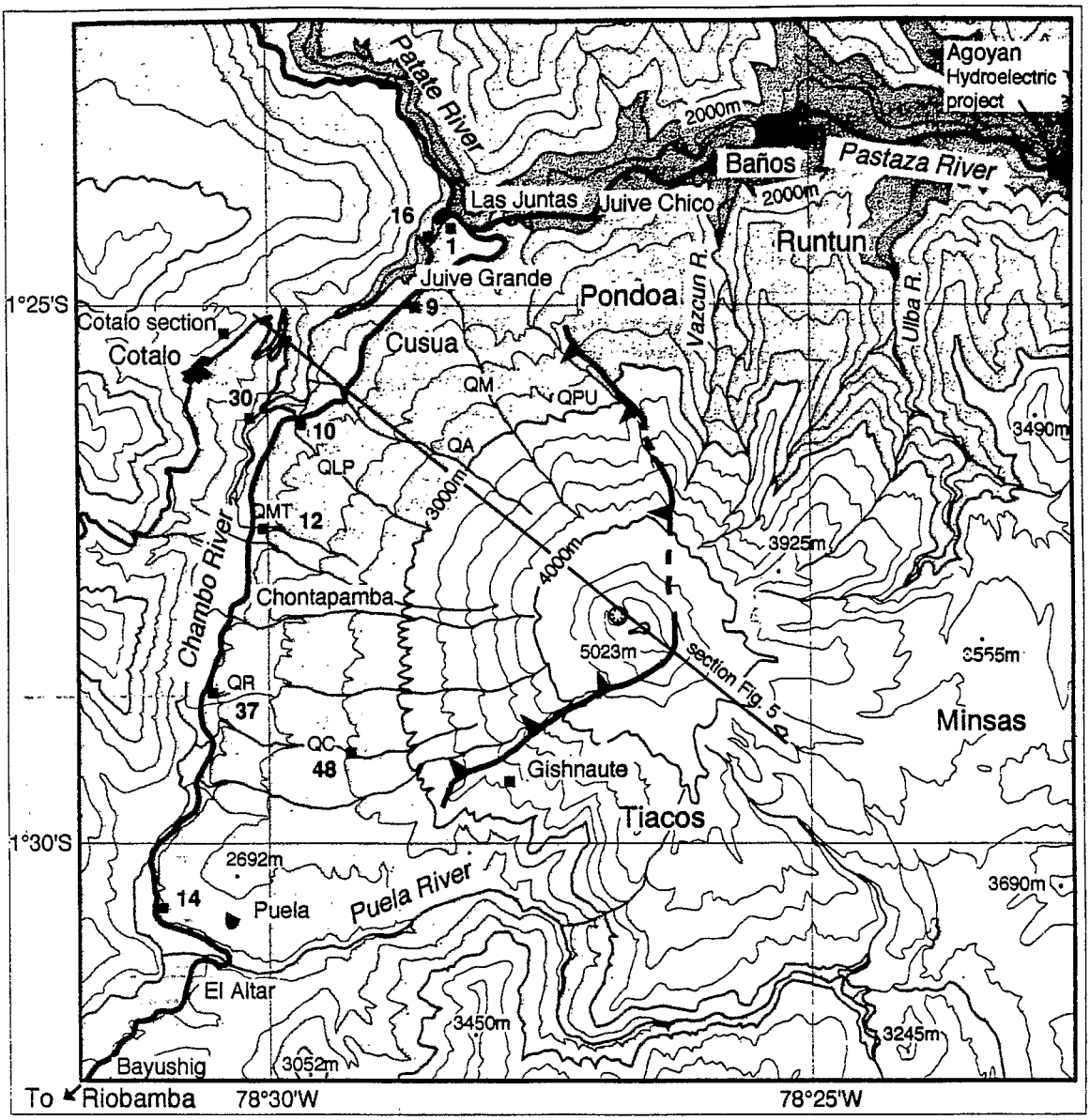

Fig. 2. Physiographic map of Tungurahua Volcano with location of sites and sections referenced in text. Bold line with teeth: avalanche caldera scar. QA = Quebrada Achupashal; QC = Quebrada Confesionario; QM = Quebrada Mandur; QMT = Quebrada Motilones; QLP = Quebrada La Piramide; QPU = Quebrada Palma Urcu; QR = Quebrada Rea. Continuous bold lines = roads.

interbedded tephra, which form the old Pondoa and Runtun surfaces, now bisected by the Vazcún valley (Fig. 3). In general, these rocks are two pyroxene andesites with or without olivine. This first stage of activity apparently culminated with sector collapses for which there is evidence in the Ulba valley and on the west side of the cone. On the upper canyon wall of the Ulba valley, a thick unit of andesitic breccias having a chaotic internal structure typical of debris avalanche deposits overlies the lava series (Fig. 4A). In addition, breccias that form several anomalous hills, up to 50 m high, are present at the western base

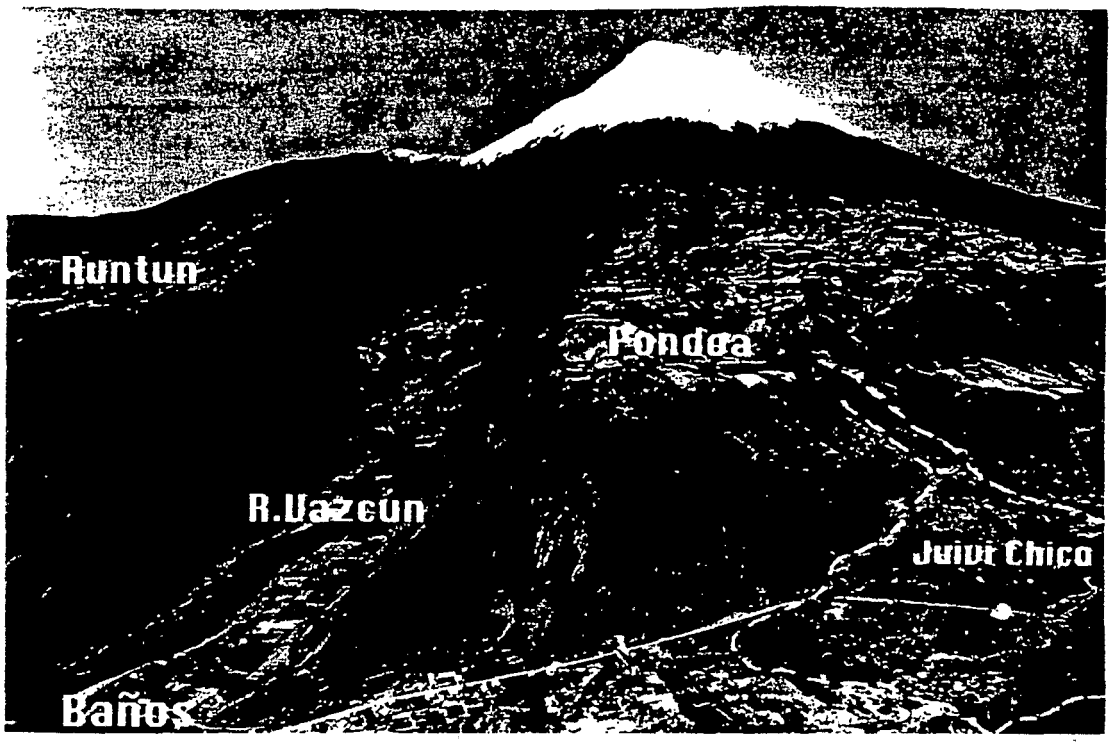

Fig. 3. Tungurahua Volcano (5023 m) as seen from the north. The deep Vazcún valley has conducted lahars and pyroclastic flows directly toward the town of Baños (1800 m) in historic eruptions.

of the cone. They consist of ~ 60 vol.% of clasts of andesitic lavas (55.8–62.3% SiO_2) and subordinate amounts of hydrothermally altered rocks; their matrix (~ 40%) is well-indurated, fine-grained ash containing abundant lithic and altered fragments. These characteristics (Siebert, 1984) suggest that these deposits are the remnant mounds of a massive avalanche related to a sector collapse that followed the Tungurahua I constructional period.

The magmatic suite of Tungurahua I varies from basic andesites to dacites (Table 1). Thick dacitic biotite-bearing lavas (Runtun dacites: 64.3–66.3% SiO_2) and subordinate dacitic block and ash flow deposits covered the avalanche deposits and are now exposed upon the Runtun surface (Fig. 4A). Similar dacitic lavas, the Minsas dacites, descended from high on the southeast slopes of Tungurahua I, and accumulated against the adjacent metamorphic hills, leaving that flank at a higher elevation than those of the north and south sides. These lavas were eroded in turn by the last important glaciation, thought to be the Late Glaciation Maximum of Clapperton (1993), placed in the interval of ~ 33,000 to ~ 14,000 years BP. Because the hydrographic network developed more rapidly on the other flanks, the southeast flank has been less eroded and better preserved. On the lower west flank, acid andesites (61.5% SiO_2) overlie the breccia sequence. Together with the Runtun and Minsas dacites, these lavas belong to an important phase of silicic volcanism that ended the long history of Tungurahua I. Andesites from Tungurahua I have given K/Ar ages of 0.77 ± 0.05 and 0.35 ± 0.04 Ma (Barberi et al., 1988).

The structure and inclination of this lava flow series clearly define the form and size of Tungurahua I. The upward projection of the original slopes converge to a hypothetical summit whose position and elevation would be similar to that of the present volcano. The downward projection of these same slopes suggests that at the end of Tungurahua I the bottom of the Pastaza valley was at about 2200 m in elevation, some 400 m higher than the present floor.

Table 1
Average compositions and individual analyses (recalculated to 100% LOI free)

	Tungurahua I			Tungurahua II		Transition II–III		Tungurahua III		
	BA (8)	AA (8)	D (5)	BA (1)	AA (15)	D (1)	BA (1)	BA (15)	AA (26)	D (10)
						TG 49	TG 48A			
SiO_2	55.75	59.04	64.93	56.60	59.71	65.70	56.23	56.47	58.66	64.51
TiO_2	1.00	0.94	0.62	0.88	0.81	0.57	0.90	0.89	0.82	0.62
Al_2O_3	17.56	16.75	16.75	16.30	16.95	16.27	17.22	16.82	16.71	16.05
$Fe_2O_3^*$	8.23	7.14	4.51	7.90	6.60	4.56	7.85	7.80	6.99	4.94
MnO	0.13	0.11	0.10	0.12	0.10	0.09	0.12	0.12	0.11	0.09
MgO	4.26	3.55	1.46	5.58	3.56	1.72	4.87	5.09	4.27	2.49
CaO	7.25	6.16	3.50	7.16	6.12	4.02	6.98	7.19	6.45	4.54
Na_2O	3.89	3.87	4.75	3.72	4.04	4.33	4.09	3.88	3.97	4.14
K_2O	1.65	2.18	3.15	1.51	1.89	2.56	1.49	1.50	1.78	2.45
P_2O_5	0.27	0.27	0.23	0.23	0.21	0.18	0.25	0.24	0.23	0.18
	100.00	100.00	100.00	100.00	100.00	100.00	100.00	100.00	100.00	100.00
FeO/MgO	1.77	1.87	2.87	1.27	1.71	2.38	1.45	1.39	1.49	1.82
Mg*	50.4	49.2	38.5	58.0	51.3	42.8	55.1	56.3	54.6	49.7
Cr	69	82	13	238	80	25	161	161	117	66
Ni	34	37	6	89	32	11	60	62	47	26
Rb	43.2	60.6	94.5	35.5	48.4	77.0	22.0	35.5	45.8	70.5
Sr	646	545	440	600	620	502	730	636	602	480
La	19.4	22.3	32.6	15.3	18.6	24.5	17.0	16.6	18.4	22.6
Yb	1.80	1.79	2.05	1.22	1.29	1.51	1.37	1.39	1.41	1.42

Numbers within brackets indicate the number of analyzed samples. BA = basaltic anderite; AA = acid andesite; D = dacite.
* Total iron as Fe_2O_3.

Thus, Tungurahua I was a normal andesitic stratovolcano, with an approximate relief of 2800 m, centered on the same conduit as the present volcano.

4.2. Intermediate cone (Tungurahua II)

Upon the upper southern flanks, the 80–100-m-thick Tiacos unit, consisting essentially of andesitic and high-Si andesitic lavas (57.7–60.7% SiO_2) and having a limited distribution, rests upon the eroded edifice of the older cone and is truncated in turn by the scarp of the sector collapse that occurred about 3000 years BP. Its unique dip and orientation suggest that it was once part of a younger cone (here called Tungurahua II) which had been constructed upon the older cone and which probably attained a similar relief (about 3000 m), given the Tiacos unit's elevation and position.

That Tungurahua II was a large and different cone is also implied by the fact that the deposits of the subsequent voluminous avalanche are composed mainly of andesitic to high-Si andesitic lavas (57.3–62.3% SiO_2) having chemical characteristics similar to that of the Tiacos series (Table 1 and Fig. 5). Furthermore, they are markedly different than those of the andesitic suite of the basal volcano, which suggests that the latter did not contribute significantly to the avalanche deposit. Thus, the Tiacos lavas are the only remaining inplace evidence of a large cone whose remnants make up the greater part of the subsequent avalanche deposit. The Tiacos activity is apparently younger than 14,000 years BP, since the Tiacos lavas occupy and post-date two glacial valleys whose terminal moraines have an elevation typical of the Late Glaciation Maximum.

4.3. Collapse of the Tungurahua II cone

Given the inferred great relief and steepness of Tungurahua II, the western flank slid readily downslope, filling the Chambo river valley with avalanche debris (Fig. 4C). The scars of the collapse amphitheater widen downslope to the west. The central part of

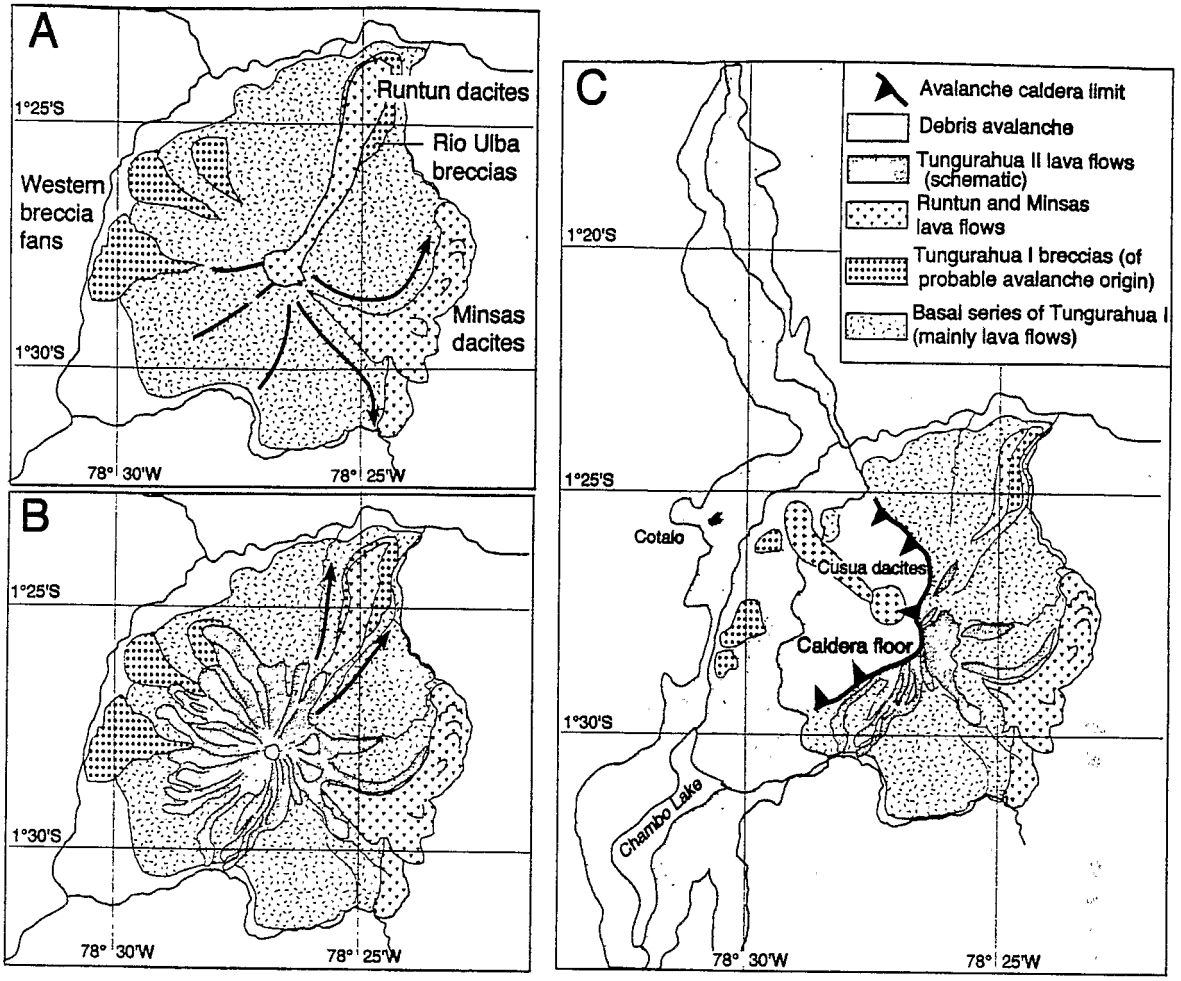

Fig. 4. Sketch diagrams showing the main periods of Tungurahua development up through the 3000-year-old avalanche event.

this avalanche collided with the high ridge immediately in front of the sector collapse. Here, thick deposits of avalanche debris were left, forming a bench upon which the village of Cotaló is presently located, some 400 m above the valley bottom (Fig. 6). The flow was also diverted to the south and the north, along the Chambo and Patate river valleys, respectively. The part of the avalanche that descended the southwest flank of the edifice did not encounter major obstacles and consequently flowed southward up the Chambo river valley. Along this path, the avalanche traveled 21 km from the presumed summit, leaving deposits and hummocks readily observed along the Baños–Riobamba road. The small village of Bayushig (Fig. 2), for example, lies within the hummocky terrain left by the avalanche. Other towns, such as Penipe, occupy terraces and abandoned stream channels that were subsequently cut into the unconsolidated breccias. The avalanche flowed up the Patate river valley for a similar distance (Fig. 4C).

The avalanche deposit is a chaotic breccia, locally monolithologic, containing 20–40% matrix of unconsolidated lithic powder, bluish-gray or pink in color. Angular clasts of andesites and high-Si andesites are the dominant fragments observed in the breccia. No stratification or internal structure is observed, except for 15–30-m-long pods of jigsaw-

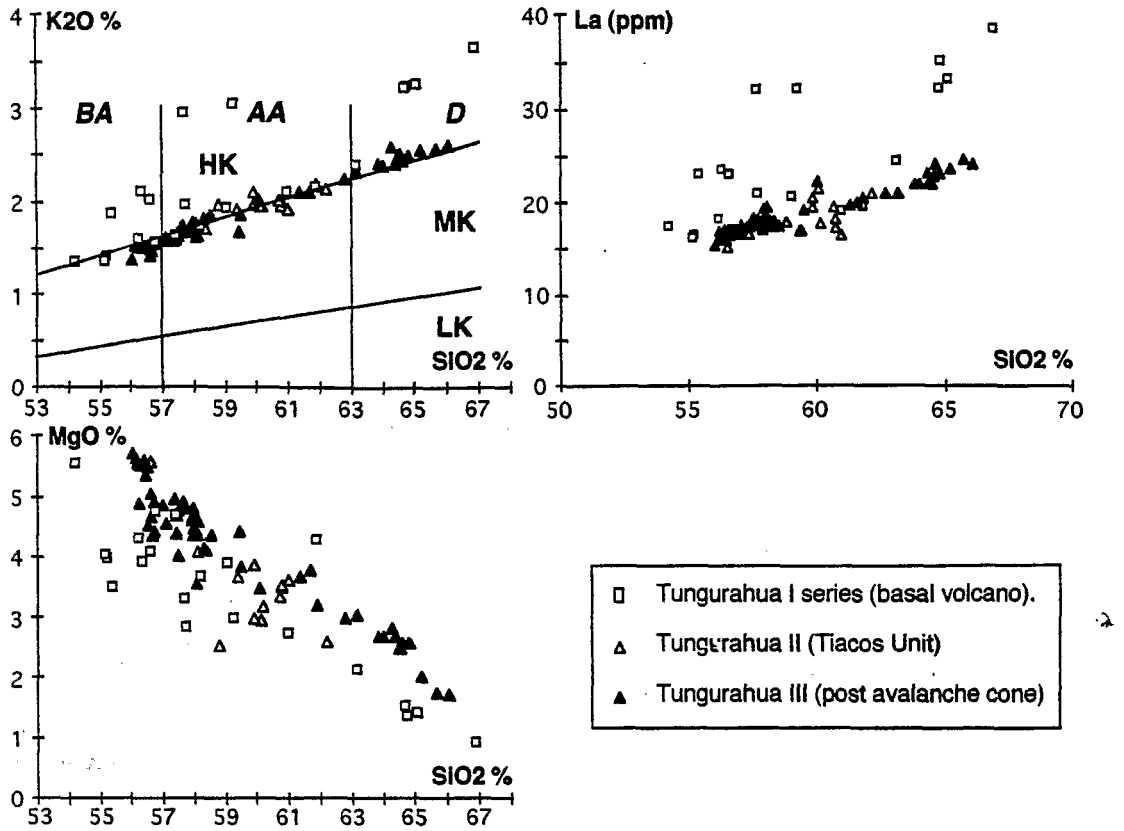

Fig. 5. K_2O–SiO_2, MgO–SiO_2 and La–SiO_2 geochemical diagrams. BA = basic andesites; AA = acid andesites; D = dacites. HK, LK and MK define the areas of high, medium and low-potassium contents.

fractured lava flows, as well as occasional packages of randomly oriented tephra sequences that contain tan to pinkish ash flow deposits with glassy dacitic blocks and/or scoria bombs. The avalanche deposit covers at least 80 km^2. Its maximum thickness at the western foot of the volcano is ~ 400 m. To the north and south, the deposit gradually thins to 30–50-m-thick, but may reach 200 m in places. Its estimated volume is ~ 8 km^3.

A large matrix-rich debris flow, yellowish-tan in color, was generated shortly after the avalanche and its deposits are seen principally in the Chambo valley where they fill depressions in the irregular surface of the avalanche deposit. Frequently, pods of unconsolidated avalanche breccia are caught up in the lahar deposit, suggesting that the lahar immediately followed the avalanche. This flow was apparently the result of the mobilization of water and ice-saturated parts of the debris avalanche, an origin similar to that of the North Fork Toutle River lahars during the 1980 Mount St. Helen's eruption (Janda et al., 1981). Scoria bombs with cooling fractures are found within the lahar, implying that an eruptive event either triggered or accompanied the collapse.

This lahar deposit overlies the main avalanche breccias on the Cotaló bench (Section, Fig. 6). Here, it contains non-carbonized logs which have been dated at 2995 ± 90 years BP, giving the age of the avalanche event. The lahar deposit is in turn overlain by a second avalanche deposit. This second avalanche must have occurred shortly after the lahar, since only an uneroded and unincised surface of the first avalanche fan would have allowed the second avalanche to cross the now deep Chambo river canyon and deposit itself upon the lahar and earlier avalanche deposits.

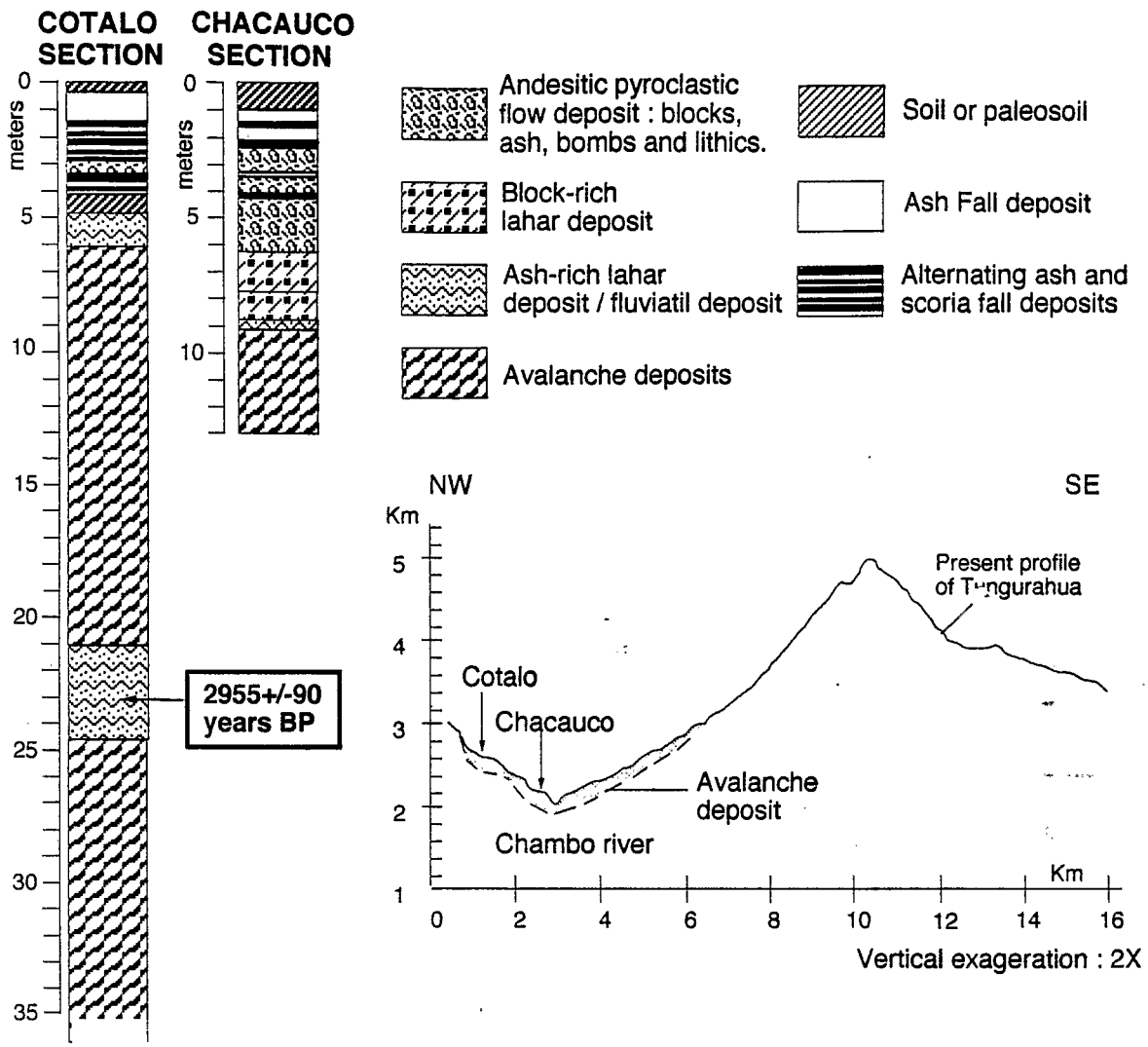

Fig. 6. NW–SE topographic profile of the present cone showing the avalanche deposit and representative stratigraphic sections in the Chambo valley.

The ~3000 years BP avalanche event was followed by the extrusion of large dacitic lava flows. South of Las Juntas, the avalanche breccia is overlain by vitrophyric dacite lavas bearing olivine, two pyroxenes and minor amphibole (the Cusua dacites, Fig. 4C; 64.0% SiO_2). These 6-km-long flows were probably related to dome extrusion in the amphitheater. A large debris flow, containing prismatically jointed glassy blocks of the same dacite, up to 10 m in size, was generated during this activity (see Fig. 9c). Following this dacitic activity, there is no evidence of eruptive activity until ~2300 years BP, implying that the volcano was quiet for approximately 700 years.

4.4. Present cone (Tungurahua III)

The past 2300 years have seen the growth of Tungurahua III, characterized by almost continuous eruptive activity and the repeated generation of lava flows, pyroclastic flows, and debris flows. These have principally descended the cone's western and

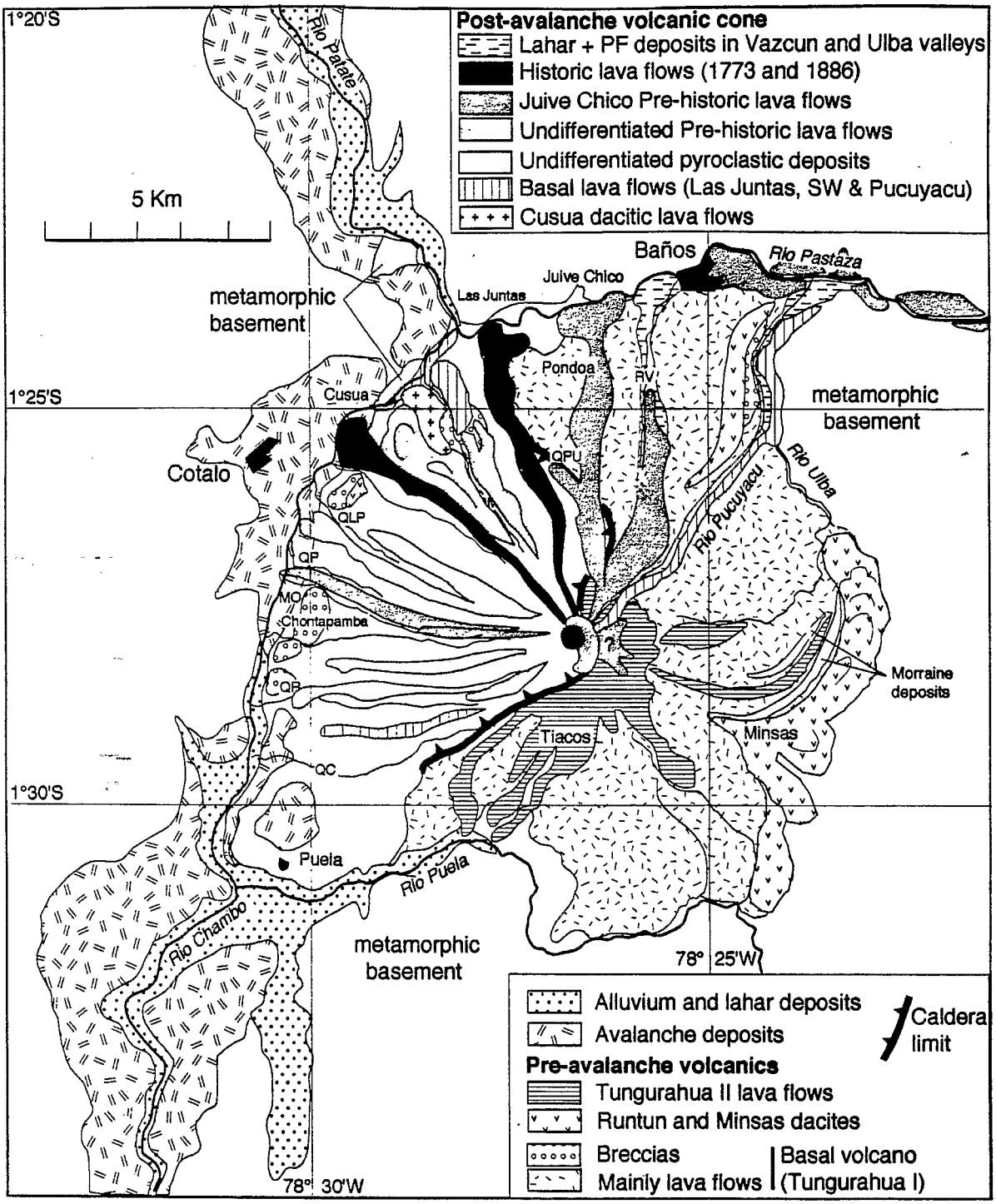

Fig. 7. Simplified geological map of Tungurahua Volcano.

northern flanks down to the Chambo and Pastaza rivers (Fig. 7). The eruptions also ejected moderate amounts of ash, scoria lapilli and occasionally pumice lapilli, which were transported by winds chiefly to

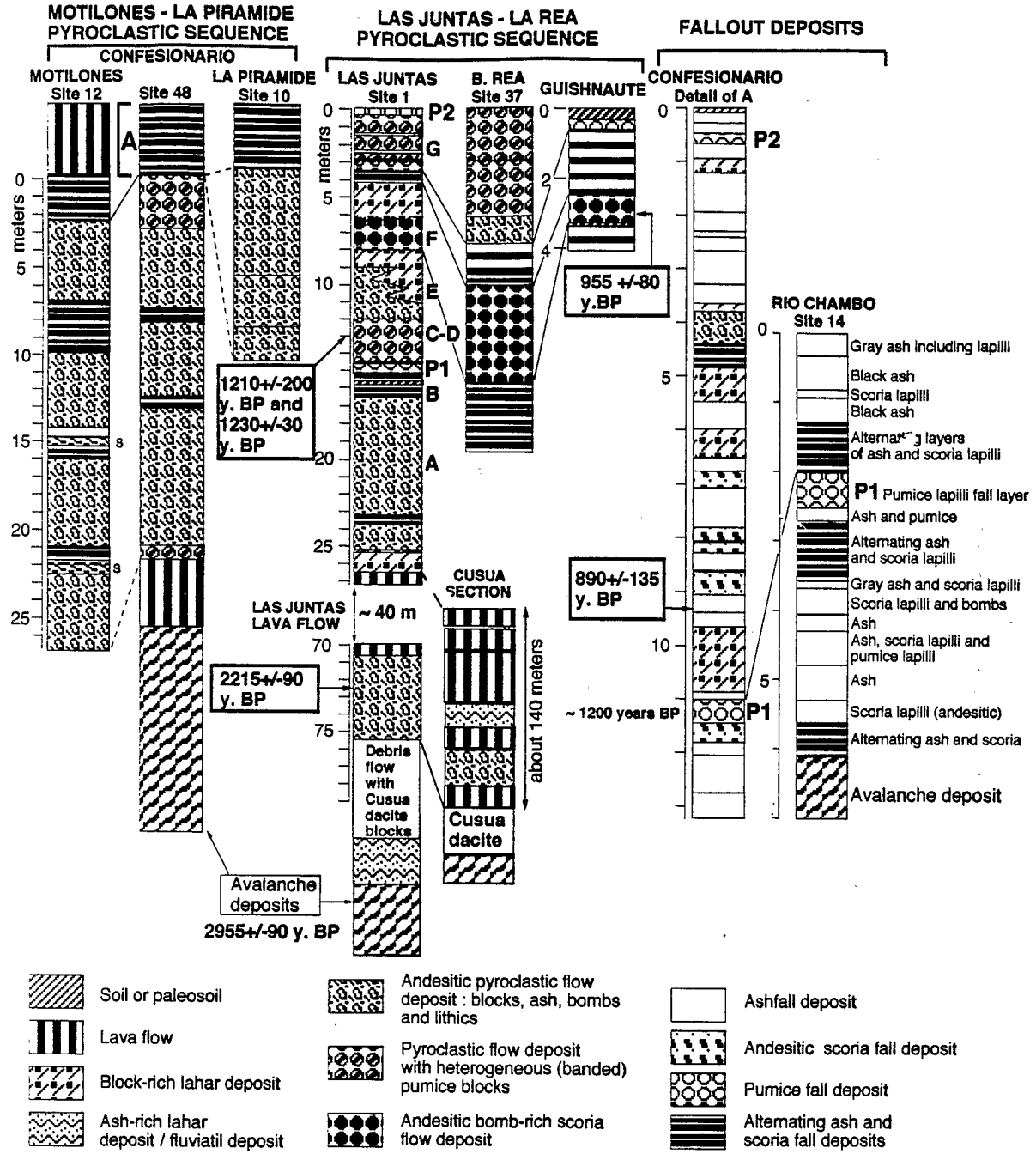

Fig. 8. Stratigraphic columns related to Tungurahua III cone. See Fig. 2 for location. Note: P1 unit marks transition from basic andesitic volcanism to mixed andesitic and dacitic volcanism. Because no soil nor hiatus is observed at this horizon, this transition was apparently rapid. Note changes in scale between columns.

the west and southwest. The Tungurahua III cone developed during two main periods (Fig. 10).

4.4.1. Tungurahua III-1

The first period (approximately 2300–1400 years BP) is composed of three volcanic units that, although discussed separately, represent a continuum of activity whose products were deposited upon different sectors of the western flank at different moments. Selected stratigraphic columns showing these deposits are presented in Fig. 8.

(1) Near Las Juntas, a series of olivine and two pyroxene basic andesite lavas (56.0–56.3% SiO_2) mark the volcano's reactivation. Most flows traveled down the west side of the new cone and then flowed 5 km northward down the Chambo valley. Interbedded in these lavas is a scoria-rich pyroclastic flow deposit of the same composition, which contains carbonized wood that has given a radiocarbon date of 2215 ± 90 years BP. The late lavas of this sequence are characterized by augite and large olivine phenocrysts (5–10 mm) and the absence of hypersthene. The total thickness of this basal unit is 140 m (see Cusua section, Fig. 8). Southwestward, in the Confesionario and La Rea valleys, similar olivine and clinopyroxene-phyric andesites occur, resting upon the avalanche debris. On the basis of petrological similarities, the lava flow which descended the Ulba valley is related to this unit.

(2) Following the basal lava series, explosive activity occurred, which led to the mantling of the new cone by thick sequences of scoria flow deposits and subordinate ash and scoria fall layers. Between the Pingullo and Confesionario channels, for example, these deposits are estimated to be > 100 m thick. They give the western side of Tungurahua III its smooth topography observed between the 2400- and 2900-m contours. On the lower slopes, the avalanche I hummocks are almost entirely covered by these deposits (as an example, see Chontapamba, Fig. 7). Stream incisions expose sections up to 30 m thick, two of which are presented in Fig. 8 (Motilones and Confesionario sections).

Pyroclastic flow and surge deposits, interbedded with thin andesitic ash and lapilli fall layers, typically contain decimeter-sized bread-crust bombs and black vitric blocks in a brown or reddish-brown ashy matrix. The juvenile clasts are invariably two pyroxene basic andesites and andesites (56.3–58.2% SiO_2). At one site (48, Confesionario valley) the basal part of the sequence shows evidence of a heterogeneous magma: juvenile andesite blocks and bombs (sample TG 48A, Table 1) contain light-gray dacitic bands and inclusions bearing amphibole (sample TG 49). These dacitic bands apparently correspond to a slightly more differentiated magma leftover from the Cusua dacitic magmatism.

In these pyroclastic flow sequences, the presence of surge deposits, numerous inclusions within the bombs, and large numbers of quenched clasts suggest powerful open-conduit explosions and magma–water interactions. The nature and shape of accessory blocks attest to the destruction of andesitic domes or lava plugs obstructing the conduit. These deposits possibly formed by collapse of the denser parts of the eruptive column, such as were observed during the brief, vertically-directed explosions generated in the 1979 St. Vincent activity (Shepherd and Sigurdsson, 1982).

During this period, block and ash flows derived from collapsing lava fronts were also produced and directed to the northwest. Their deposits are observed at La Piramide (Fig. 7 and section, Fig. 8) and in the middle of the Las Juntas section (layer A, Figs. 8 and 9a), where they predate a sequence of ash and lapilli fall layers and scoria flow deposits dated at ~ 1200 years BP. In these deposits, juvenile vitric blocks have similar compositions (56–57% SiO_2) to those encountered in the scoria flow units, showing that no significant chemical evolution occurred during this phase.

Fig. 9. Pyroclastic deposits of Tungurahua III. (a) Las Juntas section (site 1; description of layers A–G in Fig. 8 and text); (b) bomb-rich scoria flow deposit in La Rea valley, equivalent to layer F at site 1; (c) Lahar deposit in Patate valley, bearing large bombs of the Cusua dacite; (d) 1916 ash and scoria flow deposits (8-m thick) in Vazcún valley; (e) banded (andesitic and dacitic) blocks in the 1886 ash and scoria flow deposits, southeast of Las Juntas.

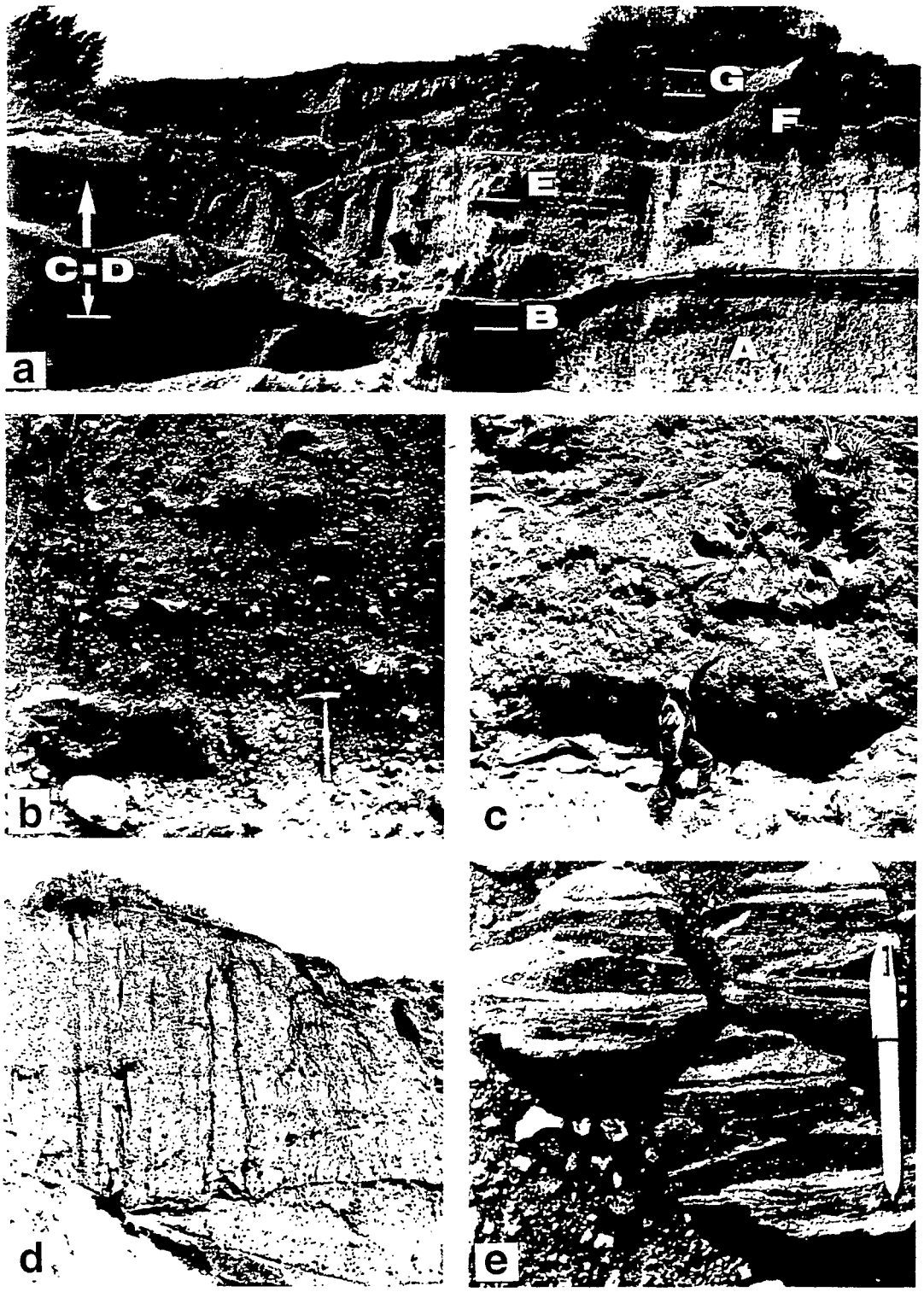
G
F
E
C-D
B
A
a
b
c
d
e

(3) A renewed phase of effusive activity followed, during which three flows of two pyroxene andesite lavas (57–58% SiO_2), whose total volume is estimated at $\sim 570 \times 10^6$ m^3, descended the northern and northwestern flanks. The main flow descended the old Pondoa surface to Juive Chico, filled the Pastaza canyon, and then flowed downvalley at least 30 km. Several towns, including Baños, sit directly upon this flow (Fig. 7). The second flow series descended the northwest flank following the Juive Grande drainage and a third flow traveled down Vazcún valley. At Pondoa, these lavas predate an ash fall layer in which charcoal gives an age of 1470 ± 85 years BP. Their youthfulness is also indicated by the well-preserved lava flow terraces, pools, and channels observed to the east of Baños.

As the dominant winds of the region blow from east to west, most tephra fell upon the western slopes of the new cone. Generally the tephra were not carried far; at sites 15 km downwind, the ash fall layers rarely exceed 10 cm. The fallout tephra of the first main period consist entirely of andesite and basic andesite products; no siliceous layers have been observed. On the contrary, significant fallout deposits of the second main period are silicic. This change is placed at a prominent pumice lapilli fall of dacitic composition (layer P1, Figs. 8 and 10) that has a wide distribution and is about 1200 years old.

4.4.2. Tungurahua III-2

The second main period of the present cone began ~ 1200 years BP and is still continuing. The upper parts of the Las Juntas section (Figs. 8 and 9a) provide a good record of the pyroclastic activity which preceded historic times. They consist of a series of pyroclastic flow deposits, fallout tephra and lahars, which begins with the P1 pumice lapilli fall (62.7% SiO_2) and scoria flow units (layers C–D) containing banded scoria bombs (61–64% SiO_2). Upsection, it continues with homogenous andesitic (57.8–58.5% SiO_2) block and ash pyroclastic flows (layers E, F), and finally ends with alternating beds of andesitic scoria lapilli and ash and banded dacitic pumice lapilli (layer G). Correlations with the La Rea and Guishnaute sequences are shown in Fig. 8. Layer F is readily recognized in most places, due to the presence of large (< 1 m) breadcrust vitric bombs.

Two radiocarbon dates on charcoal from the scoria flow deposit 1C–D were obtained from Krueger Enterprises (Cambridge, MA) and the Centre for Isotope Research (Groningen, the Netherlands); the measured ages are 1210 ± 200 and 1230 ± 30 years BP. A third date of 955 ± 80 years BP was obtained from charcoal in the bomb-rich layer at the Guishnaute section which is correlated with the F layer of the Las Juntas section and the lower layer of the La Rea section (Figs. 8 and 9b).

The eruptive style that dominated the 1200–900 years BP period returned during historic times after an apparent repose of ~ 500 years. The historic records report four eruptive periods. However, the postulated 1641 AD eruption lacks both reliable eyewitness descriptions (Egred, 1989) and stratigraphic confirmation. Thus, only three important historic eruptive periods are recognized here, each of which comprises one or more explosive episodes that mainly generated pyroclastic products of both andesitic and dacitic composition and that were followed in turn by the emission of andesite lava.

In 1773 AD, following an andesitic ash fall and a widespread dacitic pumice lapilli fall (P2 layer, 65.5% SiO_2; Figs. 8 and 10), a large andesitic lava flow, bearing augite, rare olivine and hypersthene and with an estimated volume of 102×10^6 m^3, flowed down the cone's north–northwest flank to Juive Grande and the Las Juntas area and dammed the Pastaza river for several days.

The 1886 eruption witnessed numerous pyroclastic flows that descended different routes on the western flank (Martinez, 1886), being more frequent on the northwest side, where they partially buried the 1773 lava flow. Similar to those of pre-historic eruptions, the 1886 pyroclastic flows (basically ash and scoria flows) contain well-banded bombs whose composition ranges from acid andesites to dacites (61–64.5% SiO_2; Fig. 9e). Plagioclase, augite, hypersthene, olivine and a trace of amphibole comprise the typical mineralogy of the acid andesites. A few months later, a lava flowed down the northwest flank towards Cusua and dammed the Chambo river; its volume is estimated at 89×10^6 m^3. This lava has the same composition (61.3% SiO_2) as the less silicic bombs of the preceding pyroclastic flows, but is more siliceous than the lava left in the crater by the 1916–1918 activity.

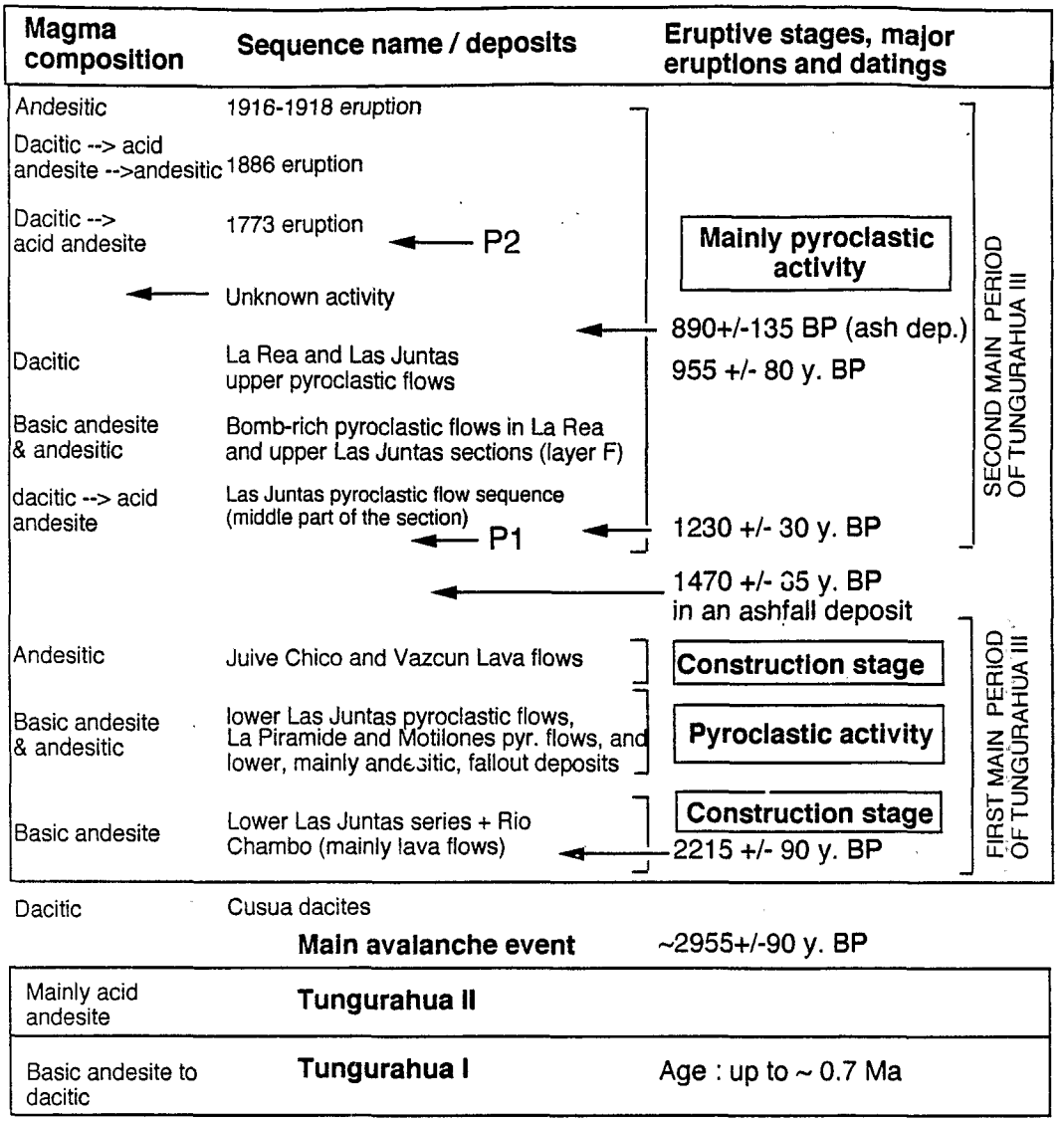

Fig. 10. Generalized stratigraphy of Tungurahua volcano with special emphasis to the post avalanche Tungurahua cone.

Finally, the 1916–1918 eruptive episode was most noteworthy for the numerous pyroclastic flows which descended the northwest and north flanks to the Las Juntas area and Vazcún valley (Fig. 9d); many were witnessed and photographed (Martinez, 1932). The composition of these products was mainly andesitic (56.8–57.7% SiO_2). During this episode, lava was also confined to the crater.

Lahars were produced during the 1773, 1886 and 1916–1918 eruptions. Baños narrowly escaped disaster in 1773, when a large debris flow in the Vazcún valley barely spilled over into the city. In 1886, the largest lahars descended the SW flank to Puela. Others traveled down the Vazcún and Ulba valleys, which again saw large lahars during the 1916 eruption.

5. Discussion and conclusion

5.1. Emplacement of the 3000-year-old avalanche

The characteristics of the 3000 years BP debris avalanche are worthy of further discussion, given its youthfulness, good preservation, and notable size. Factors that played a dominant role in the distribution of the deposits include: its large volume (estimate 8 km^3), the great relief (estimate 3000 m) and steep slopes (25–35°) of the cone, and the intrusion of dacitic magma into the cone which apparently led to its instability, a situation similar to that of the 1980 Mount St. Helens event (Voight et al., 1981).

In order to better document the nature of the collapse, the event was modeled as follows. The western flank of the cone was divided into three sectors, to take into account the differences in the presumed topographic relief. The northwest flank is thought to have had ~3000 m of relief, the west flank, some 2800 m of relief, and the southwest side about 2600 m of relief. Fig. 11 shows that an avalanche with $H/L = 0.11$ best fits the overall distribution and reach of the 3000-year old deposits in the Patate and Chambo valleys. Based upon this theoretically possible distribution and our field observations, we surmise the following scenario.

The main axis of the collapse was to the northwest. There, the high ridge of La Piramide helped to split the avalanche into two parts. The part which traveled south of this ridge collided directly with the canyon wall near Cotaló, in agreement with the thickest avalanche deposits (±400 m) observed in the Chambo valley. Part of this flow surmounted the canyon wall and was diverted to the north–northeast by the lower slopes of Cerro Huisla toward the Patate valley (arrow 1, Fig. 11). There, deposits up to 50 m thick are still preserved as far as 15 km up the valley. Additionally, a part of the avalanche traveled north of La Piramide ridge and was funneled up the axis of the Patate valley (arrow 2). Southwestwards, the avalanche flowed up the Chambo river valley about 15 km, taking advantage of its flat gradient.

An unusual characteristic of the Tungurahua avalanche event is its widely open (~110°) amphitheater. Considering the orientation of collapse amphitheaters to tectonics, sector collapses in the Andes tend to occur perpendicularly to regional faults (Francis and Wells, 1988). This is the case at Tungurahua, where the main tectonic lineaments are oriented NNE–SSW and NNW–SSE. The southern limit of the avalanche amphitheater is bounded by a northeast-trending fault, while its northwest-oriented northern limit is aligned with a possible fault in the Patate valley. Among the Andean volcanoes, only the collapse of the Old Cone of San Pedro Volcano, cut by an NNW–SSE striking normal fault, seems to have generated such a wide depression. Thus, although the deformation related to the intrusion of a viscous cryptodome probably triggered the avalanche, as suggested by the post-collapse extrusion of dacite lavas, the local tectonic pattern apparently played an important role in orienting the collapse event. At least it was a key factor in controlling the width and shape of the avalanche amphitheater.

5.2. Variable eruptive behavior of the Tungurahua III activity

The activity of Tungurahua III has had variable eruptive styles and corresponding products. The available information about historic eruptions, as well as that obtained from field work, suggests that this activity has had a cyclic pattern, alternating between explosive and effusive episodes, during both the first and second periods.

During the first period of Tungurahua III, from 2300 to 1400 years BP, the two major effusive episodes (the Las Juntas lava sequence and later the Juive Chico lava outpouring) were separated by large pyroclastic episodes (e.g., the Motilones and La Piramide scoria flow sequences). Despite this variation in behavior, no significant petrological evolution is noted; that is, the eruptive products have varied little in composition (SiO_2 55–58%) during about 1000 years. This, in turn, suggests that magma was probably supplied almost continuously from a deep source and consequently little differentiation occurred in whatever shallow magma chambers might have existed. Variable magma/water ratios, as suggested by the phreatomagmatic character of the Tungurahua III-1 pyroclastic deposits, would best explain this variation in eruptive style. For example, until the pyroclastic episode of Tungurahua III-1, the volcano probably had a lower elevation and a limited icecap, resulting in a less phreatomagmatic and a more

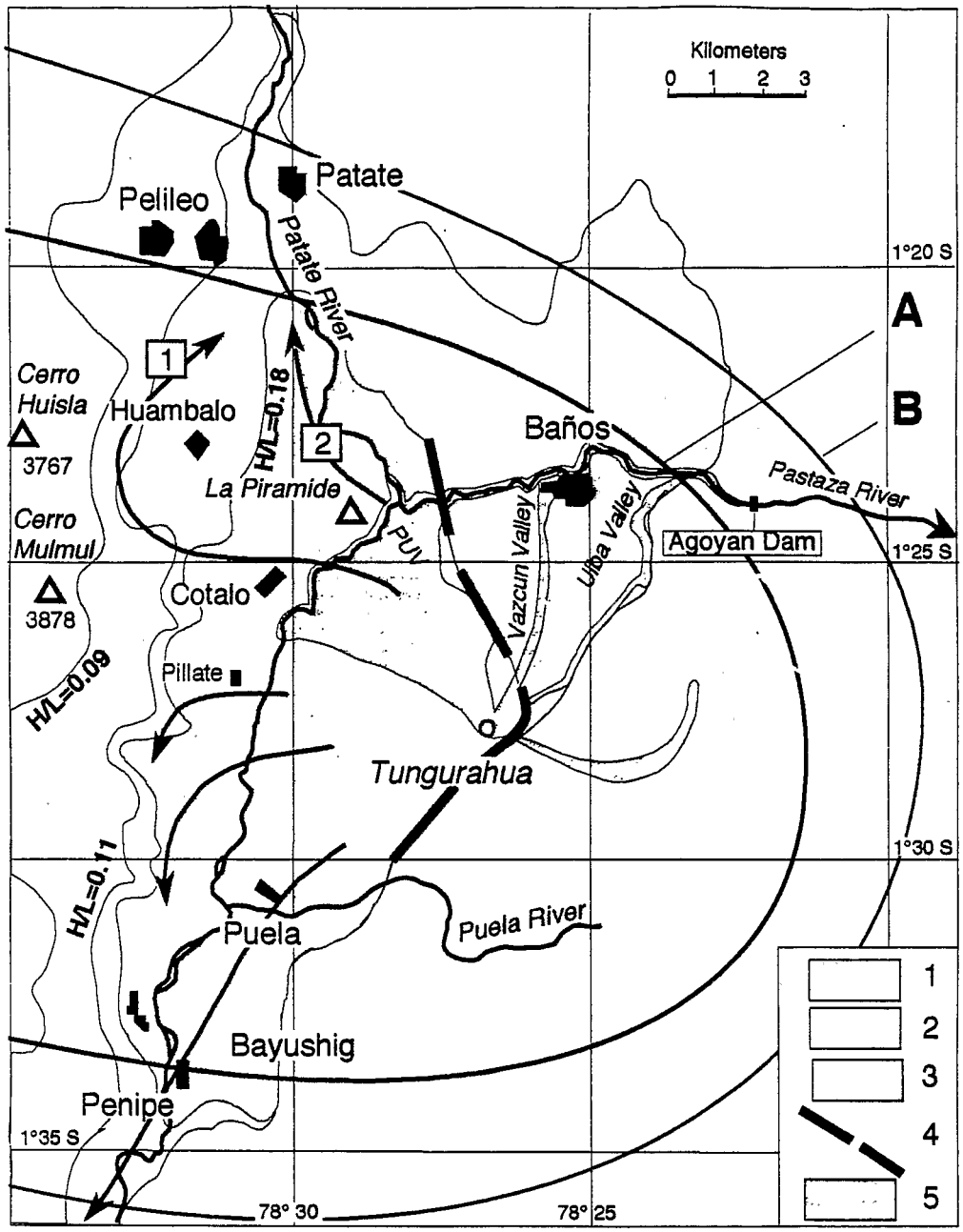

Fig. 11. Hazard map for lava flows, fallout deposits and sector collapse events. 1 = Distribution of a hypothetical debris avalanche with an $H/L = 0.09$; 2 = distribution of a hypothetical debris avalanche with an $H/L = 0.11$, very similar to the 3000 years BP avalanche; 3 = distribution of a hypothetical debris avalanche with an $H/L = 0.18$ (small volume avalanche); 4 = caldera limits which would control the distribution of small- to medium-size avalanches in future events; 5 = most probable paths of future lava flows. Expected ash fall distributions: $A < 10$ cm; $B < 5$ cm.

effusive behavior. As the volcano attained a greater height during Tungurahua III-2 and supported a larger icecap, phreatomagmatic activity became progressively more important.

Beginning about 1300 years BP, the activity of Tungurahua III-2 has been characterized by repetitive pyroclastic episodes (tephra falls and pyroclastic flows) followed by lava flows or crater plugs. Pyroclastic activity dominates the main part of each eruptive episode, thanks to the role played by both juvenile and meteoric water. However, as the volcano heats up and dries out, less meteoric water is available and more effusive activity ensues. This leads to lava flows, dome extrusion, and block and ash flows. This cyclic process is similar to that observed in many andesite volcanoes, (e.g., Fuego de Colima in Mexico; Robin et al., 1991). Parallel to the eruptive evolution, a petrologic evolution is noted in the course of these eruptive cycles. From mainly acid andesite to dacitic at the beginning of the eruptive cycles, the magma turns andesitic with the lavas emitted at the end of the eruptions.

These eruptive events occur approximately every 100 years, which roughly agrees with the number of eruptive sequences observed for the past ~1300 years as well as with the eruption frequency of the past 300 years.

5.3. Growth rate of the present cone

The good chronological control as well as the well constrained topographic changes permit an estimate of the magma flux at Tungurahua. During the growth of Tungurahua III, the point of emission has not varied, which has had the effect of directing the greater volume of its volcanic products into constructing the new cone within the amphitheater.

Earlier, we estimated the volume of the avalanche deposits at ~8 km^3. This corresponds to an avalanche depression of ~6 km^3, taking into consideration the expansion effect noted by Voight et al. (1981) for the Mount St. Helens avalanche deposit. Given the height of the amphitheater scars (30–160 m high) and the present slopes of ~30°, we calculate that ~3.1 km^3 of material is still needed to rebuild the cone to its previous height. Thus, the approximate volume of the present cone is 2.9 km^3. Considering that the cone is roughly composed of 70% pyroclastic deposits (mean density 1.6) and 30% lava flows (density ~2.65), such a volume represents ~2 km^3 DRE. To this volume, we add the 0.57 km^3 of lava that flowed out of the caldera (Juive Chico series) and the estimated 0.85 km^3 (DRE) of tephra that fell downwind of the volcano, the latter being based upon a 20×40 km elliptic distribution pattern with a maximum combined ash fall thickness of 8 m at the cone. Thus, we estimate that the magma flux (DRE) has been about 3.45 km^3 during 2300 years, corresponding to a magma supply rate of about 1.5×10^6 m^3/year.

This rate is similar to the rates given by K. Nakamura (1964) and M. Nakamura (1967) for the last 1500 years at Oshima Volcano and for the period 4000–1000 years BP at Kaimon-dake Volcano (1.67×10^6 m^3/year and 1.17×10^6 m^3/year, respectively). Our estimate also fits in the range of construction rates for andesitic volcanoes: from 0.63×10^6 m^3/year (Hakone Volcano) to 2.7×10^6 m^3/year (Sakurajima Volcano), although the contribution of dispersed tephra was not considered in those calculations (Nakamura, 1976; Wadge, 1982). The present value is also similar to the cumulative volume of lavas produced at Merapi Volcano during the last century (1.2×10^6 M^3/year, Siswowidjoyo et al., 1995). Conversely our estimate at Tungurahua for the last 2300 years is 2–3 times the estimated rate of eruptive volume in the Central Andes for the Late Cenozoic (Baker and Francis, 1978; Crisp, 1984). The intermittent character of andesitic magmatism is well known elsewhere: this implies that Tungurahua's activity has been intense during the past 2300 years.

5.4. Volcanic hazard assessment

5.4.1. Hazards due to sector collapses and related lahars

Although a sector collapse and associated debris avalanche are rare events, at Tungurahua they have occurred at least twice in the geologic past and the most recent event happened only 3000 years ago. Collapse events repeated at relatively short time intervals are reported for several andesitic edifices, (e.g., Augustine Volcano in Alaska, Siebert et al., 1995).

In Fig. 11, three sizes of avalanches are considered: (1) an avalanche with $H/L = 0.11$, characteristic of large volume avalanches (Siebert et al., 1987); (2) a worst case event (greater runout and a $H/L = 0.09$); and (3) an avalanche with $H/L = 0.18$, a

value typical of small avalanches (< 1 km^3). Due to the rapid supply of magma during the last 2300 years, Tungurahua Volcano has already refilled about half of the avalanche depression. Thus, it is believed that the conditions of the present cone (3000 m relief and 30° slopes) will favor a future collapse. If it were to happen today, an avalanche of 1–3 km^3 in volume could be generated and would have a distribution similar to that shown in case 3.

Lahars associated with collapse events generally form by the remobilization of water-saturated parts of the avalanche deposits, or by the incorporation of water and snow (Gorshkov, 1959; Janda et al., 1981). Furthermore, lahars may occur during or after eruptions when lakes dammed by avalanche debris break out catastrophically, or when a large volume of water is displaced violently (Glicken et al., 1983; Meyer et al., 1986; Siebert et al., 1987).

Following the 3000-year old avalanche event, a 14-km long section of the Chambo river valley was blocked by the avalanche debris and associated lahar deposits, forming a large natural dam and a ~ 10-km-long lake (Fig. 4C). This temporary lake, whose volume is estimated at 0.4 km^3, left a ~ 19-m-thick sequence of finely-bedded lacustrine sediments, mainly gray sands and silts, that are found up to the

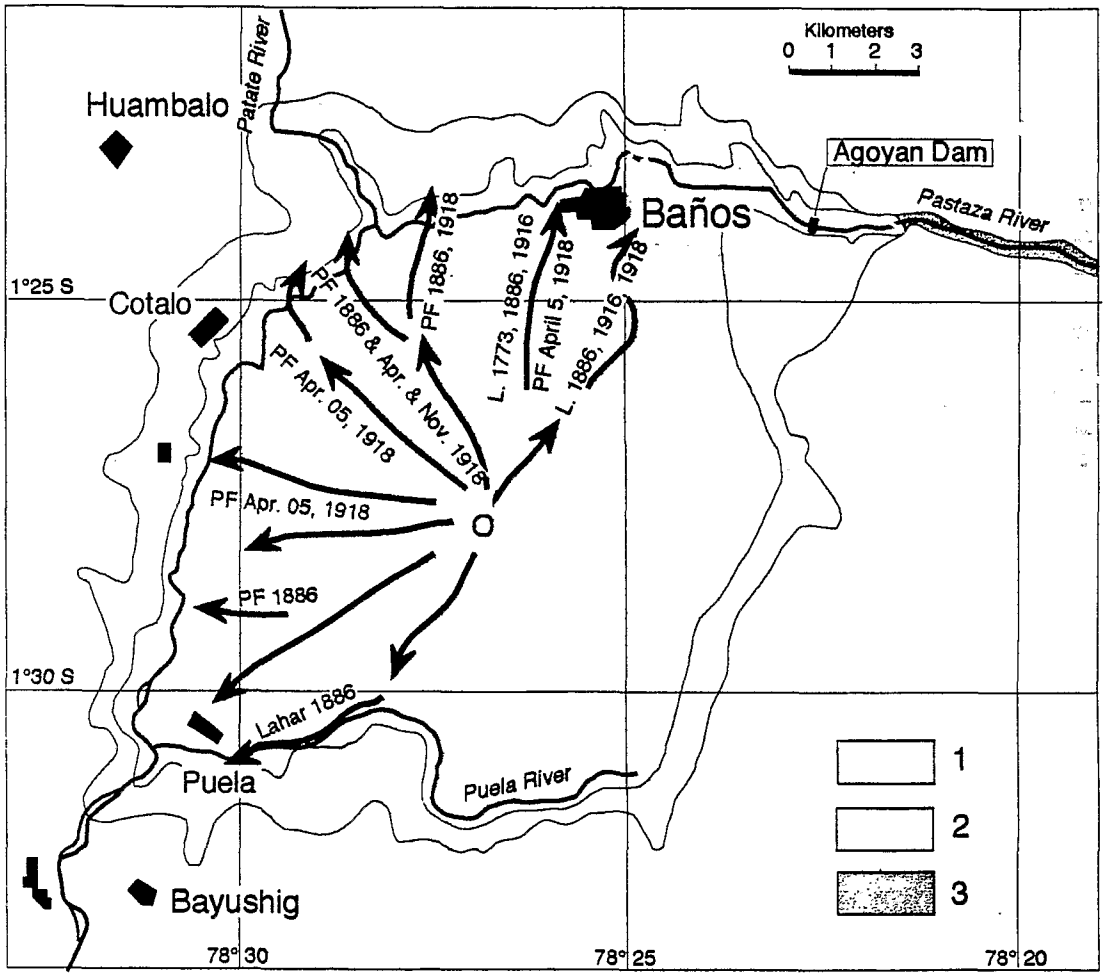

Fig. 12. Hazard map for pyroclastic flows and lahars, showing the main runouts followed by historic flows (PF = pyroclastic flows). 1 = High hazard for directed blasts and fallback pyroclastic flows over the whole area, and lahars in the valleys; 2 = minor hazard area for pyroclastic flows; 3 = high hazard for lahars in the lower Pastaza valley.

2410-m contour line in the Puela and Chambo river valleys. As the rising lake in the Chambo valley topped and breached the natural dam, the resulting flood generated an enormous debris flow that left thick, localized deposits containing avalanche breccia pods and andesitic clasts in a gray sandy matrix, derived from the reservoir sediments. At Las Juntas, the avalanche deposits are buried by this debris flow unit which in turn is covered by the dacite-block lahar associated with the Cusua dacitic lava extrusion. This clearly indicates that the lake-breakout debris flow is one of the events of the avalanche cycle. At the confluence of the Pastaza and Topo rivers, 30 km downstream from Baños, a similar deposit, up to 120 m thick, is observed. Its thickness emphasizes the catastrophic nature of this laharic event.

Following an avalanche event, lahars certainly represent the greatest hazard and this hazard remains high long after the eruption has ended, especially when large drainages are blocked and lakes are formed. Some of the largest lahars probably resulted from lake breakouts (Siebert et al., 1987). Tungurahua's setting invites such a possibility: even if the next collapse is of small volume (< 1 km^3), the resulting debris avalanche would likely refill the narrow Chambo valley, damming it, which would probably generate another lake-breakout debris flow of significant proportions.

5.4.2. Hazards due to lava flows, pyroclastic flows and associated debris flows

Due to the relatively high viscosity of the magmas, lava flows do not attain great velocities and thus do not represent a major hazard for populations living at the foot of the volcano (Fig. 11).

From the study of historic and prehistoric activity it is clear that pyroclastic flows and lahars triggered by pyroclastic flow/surge activity represent the principal hazards. Based upon the eruption frequency of the last 2 millenniums, future eruptions are to be expected and consequently, the emission of pyroclastic flows and lahars such as occurred in 1886 and 1916–1918 are likely. In this case, Baños and several villages located on the western and northern flanks would be directly threatened. Fig. 12 emphasizes the pyroclastic flow and debris flow hazards in the valleys which head on the volcano, especially the Vazcún and Ulba valleys, which descend toward Baños and the Agoyan dam.

Acknowledgements

This study is part of a cooperative program in volcanology carried out by the Geophysical Institute of the National Polytechnical School of Quito and IRD (French Scientific Research Institute for the Development in Cooperation, ex-ORSTOM). Five ^{14}C datings were done by Krueger Enterprises (Cambridge, MA) and one additional dating by Dr. J. van der Plicht at the Centre for Isotope Research, University of Groningen (the Netherlands). Thanks are also due to Jo Cotten (Université de Bretagne Occidentale, Brest, France) for providing the whole-rock analyses. The final version of the paper was greatly improved by the careful reviews by S. De Silva and an anonymous reviewer.

References

Almeida, E., Ramon, P., 1991. Las erupciones historicas del volcan Tungurahua. Bol. Geol. Ecuat. 2 (1), 89–138.

Baker, M.C.W., Francis, P.W., 1978. Upper Cenozoic volcanism in the Central Andes—Ages and volumes. Earth Planet. Sci. Lett. 41, 175–187.

Barberi, F., Coltelli, M., Ferrara, G., 1988. Plio–Quaternary volcanism in Ecuador. Geol. Mag. 125 (1), 1–14.

Clapperton, C.M., 1993. Quaternary Geology and Geomorphology of South America. Elsevier, Amsterdam, 779 pp.

Crisp, J.A., 1984. Rates of magma emplacement and volcanic output. J. Volcanol. Geotherm. Res. 20, 177–211.

Egred, J., 1989. Informe sobre la investigacion historica referente a las erupciones de los volcanes Tungurahua y Cotopaxi. In: Proyecto hidroelectrico San Francisco: informe Final de vulcanologia, Unpublished report. Republica del Ecuador, Ministerio de Energia y Minas, Sept. 1989, 123 pp.

Francis, P.W., Wells, G.L., 1988. Landsat thematic mapper observations of debris avalanche deposits in the Central Andes. Bull. Volcanol. 50, 258–278.

Glicken, H., Meyer, W., Carpenter, P.J., Sabol, M.A., Swift, C.F., Kresh, D.L., 1983. Actual and potential lake breakouts at Mount St. Helens, Washington. Eos, Trans. Am. Geophys. Union 64, 894, abstract.

Gorshkov, G.S., 1959. Gigantic eruption of the Volcano Bezymianny. Bull. Volcanol. 20, 77–109.

Hall, M.L., Hillebrandt, C.G., 1988. Mapa de los peligros volcanicos potenciales asociados con el volcan Cotopaxi. 1/50.000 scale map, in two parts (north and south), Republic of Ecuador.

Instituto Geofisico de la Escuela Politecnica Nacional (Ed.), UNDRO-USAID-EPN Project.

Hall, M.L., Vera, R., 1985. La actividad volcanica del volcan Tungurahua: sus peligros y sus riesgos volcanicos. Rev. Politec., Quito 10, 91–144.

INECEL (Instituto Ecuatoriano de Electrificacion), 1989. Proyecto hidroelectrico San Francisco: informe Final de vulcanologia. Unpublished report. Republica del Ecuador, Ministerio de Energia y Minas, Sept. 1989, 123 pp.

Janda, R.J., Scott, K.M., Nolan, K.M., Martison, H.M., 1981. Lahar movement, effects, and deposits. In: Lipman, P.W., Mullineaux, R. (Eds.), The 1980 Eruptions of Mount St. Helens, Washington. Geological Survey Prof. Papers 1250, pp. 461–486.

Litherland, M., Egüez, A., 1993. Mapa geológico de la República del Ecuador, 1/1.000.000. British Geological Survey (Keyworth, Nottingham) y CODIGEM (Quito, Ecuador), Quito.

Meyer, W., Sabol, M.A., Glicken, H., Voight, B., 1986. The effects of ground water, slope stability and seismic hazards on the stability of the South Fork Creek blockage in the Mount St. Helens area, Washington. US Geol. Survey Prof. Paper 1345.

Martinez, A., 1886. Report in the La Nacion newspaper, 17 March 1886, Guayaquil.

Martinez, N., 1932. Las grandes erupciones del Tungurahua de los años 1916–1918. Publicaciones del Observatorio Astronomico de Quito, Seccion de Geofisica, Quito (Ecuador).

Nakamura, K., 1964. Volcano-stratigraphic study of Oshima volcano, Izu. Bull. Earthquake Res. Inst. Tokyo Univ. 42, 649–728.

Nakamura, K., 1976. Preliminary estimate of global volcanic production rate. In: Colp, J.L. (Ed.), The Utilization of Volcano Energy, Sandia Laboratories, Albuquerque, pp. 273–285.

Nakamura, M., 1967. On the volcanic products and history of Kaimon-dake volcano. Bull. Volcanol. Soc. Jpn. 12, 119–131.

Reiss, W., 1874. Über lavaströme der Tungurahua und Cotopaxi. Zeitschr. Dt. Geol. Ges. 26, 907–927.

Reiss, W., Stübel, A., 1904. Das Hochgebirge der Republik Ecuador, Petrographische Untersuchungen, Berlin, 236 pp.

Robin, C., Camus, G., Gourgaud, A., 1991. Eruptive and magmatic cycles at Fuego de Colima volcano. J. Volcanol. Geotherm. Res. 45, 209–225.

Salazar, E., 1977. La geologia del flanco septentrional del volcan Tungurahua. Tesis de grado, Escuela Politecnica Nacional, Quito, 98 pp.

Shepherd, J.B., Sigurdsson, H., 1982. Mechanism of the 1979 explosive eruption of Soufrière volcano. J. Volcanol. Geotherm. Res. 13, 119–130.

Siebert, L., 1984. Large debris avalanches: characteristics of source areas, deposits and associated eruptions. J. Volcanol. Geotherm. Res. 22, 163–197.

Siebert, L., Glicken, H., Ui, T., 1987. Volcanic hazards from Bezymianny- and Bandai-type eruptions. Bull. Volcanol. 49, 435–459.

Siebert, L., Begét, J.E., Glicken, H., 1995. The 1883 and late-prehistoric eruptions of Augustine Volcano, Alaska. J. Volcanol. Geotherm. Res. 66, 367–395.

Simkin, T., Siebert, L., 1994. Volcanoes of the World, 2nd edn. Smithsonian Institution, p. 142.

Siswowidjoyo, S., Suryo, I., Yokoyama, I., 1995. Magma eruption rates of Merapi volcano, Central Java, Indonesia during one century (1890–1992). Bull. Volcanol. 50, 111–116.

Stübel, A., 1886. Skizzen aus Ecuador. Asher edn., Berlin, 176 pp.

Voight, B., Glicken, H., Janda, R.J., Douglass, P.M., 1981. Catastrophic rockslide, avalanche of May 18. In: Lipman, P.W., Mullineaux, R. (Eds.) The 1980 Eruptions of Mount St. Helens, Washington. Geological Survey Prof. Papers 1250, pp. 347–378.

Wadge, G., 1982. Steady state volcanism: evidence from eruption histories of polygenic volcanoes. J. Geophys. Res. B 87 (5), 4035–4049.

Wolf, T., 1892. Geografia y geologia del Ecuador, Brockaus edn. Leipzig, 671 pp.